BI-DIRECTIONAL VARIATION OF LATERAL STIFFNESS IN A 100MM×100MM×24MM SQUARE SHAPED SCRAP TIRE RUBBER BASE ISOLATOR WITH PARTIAL BONDING

Md. Mistak Hossain*[1] and Samiya Rahman Oishee[2]

[1]*Graduate Student, North South University, Bangladesh, e-mail: mdmistakabir786@gmail.com*
[2]*Student, Brac University, Bangladesh, e-mail: samiya.rahman.oishee@g.bracu.ac.bd*

***Corresponding Author**

ABSTRACT

This paper focuses on shear deformation and horizontal cyclic stiffness associated with seismic performance of Scrap Tire Rubber Pad isolators having various bonding levels using bi-directional loading. Scrap Tire Rubber Pad Base Isolators made from recycled tires, are a cost-efficient and eco-friendly alternative for outskirts/rural areas or seismically active sites. Using MSC Marc-Mentat FEA analysis to evaluate the isolators' flexibility and energy absorption, they are tested at various loading angles and bonding levels (0%, 25%, 50%, 75% and 100%). The results demonstrate that unbonded STRP has broad hysteresis loops and good flexibility. However, properly bonded STRP-100 exhibits superior rigidity and minimal deformation in comparison, particularly for greater loading direction and displacement angles. Lateral stiffness decreased with percentage of bonding until it comes to 75% and fully bonded shows the highest. The advantages of partial bonding are demonstrated by partially bonded models' varied stiffness under various loading orientations and displacements. Though stiffness is founded in a big margin in this study than other dimension based square shaped model. These findings imply that buildings requiring greater stiffness benefit most from fully bonded STRP isolators. On the other hand, half bonded STRP isolators work better in situations when design flexibility is needed.

Keywords: *Lateral Stiffness, Base Isolator, Seismic Performance, Hysteresis loop, FEA*

1. INTRODUCTION

Base-isolation is a widely employed technique to protect buildings from earthquake damage. One of the elements used in this case is Steel-reinforced elastomeric isolators. However, the use of Steel-reinforced elastomeric isolators in public buildings and masonry structures is limited due to the high price and high weight. It is necessary to develop a cheap isolator that can be utilized by following the standard design pattern instead. Scrap tire rubber pad isolator can be a good option as a base isolator (Turer & Özden, 2007), (Kalfas et al., 2020). As a result, we can expect the STRP isolator to behave much like the SREIs because tires are produced by vulcanizing rubber having steel cables imbedded in them. An experiment confirmed that the ratio of the vertical-to-horizontal stiffness of a STRP isolator is 450-600 (Mishra, 2012) as well. Moreover, the shear modulus of the tire rubber is about 1.0 MPa which is the AASHTO-LRFD Specification range for natural rubber 0.55-1.20 MPa (Turer & Özden, 2007), (Mishra, 2012).

An STRP isolator without mechanical bonding to the structural components is considered more beneficial. The rollover deformation of an unbonded STRP isolator helps prevent significant elastomer tension, also a fully bonded isolator shows maximum stiffness, and partially bonded worked very well (Zisan & Igarashi, 2022). Additionally, reducing lateral stiffness increases rollover deformation and thereby enhances base isolation efficiency (Zisan & Igarashi, 2021). The performance of STRP isolators and STRP base-isolated buildings under lateral stress was evaluated in earlier research (Zisan & Igarashi, 2021) (Zisan & Igarashi, 2022). Zisan and Igarashi evaluated the stress-strain behaviour of an unbonded STRP isolator under lateral load (Zisan & Igarashi, 2021). For horizontal stiffness, a hysteresis force model has been created and assessed under uniaxial lateral stress (Zisan et al., 2022). These investigations were conducted along the isolator's primary axis under uniaxial lateral load. It is crucial to examine the unbonded STRP isolator under various lateral load orientations, as lateral forces are bidirectional. It is necessary to examine how loading directionality affects lateral load performance when an isolator is used without, partially and fully mechanical fastening. Thus, this study focused on how the loading direction affected the lateral load performance of the unbonded, partially and fully bonded STRP isolator. Six loading orientation scenarios 0°, 15°, 30°, 45°, 60°, 75° are examined for Square-shaped isolators measure 100mm × 100mm × 24 mm.

2. SCRAP TIRE RUBBER PAD BASE ISOLATOR

Mishra (Mishra, 2012) describes how to build a Scrap Tire Rubber Pad (STRP) layer. The STRP isolator used in this study was made from Bridgestone 385/65R22.5 tires. It is composed of five layers of reinforcement, each 12 mm thick. As seen in Fig. 1(b), these reinforcing layers are oriented at a ±70° angle to the steel carcass. Fig. 1(a) illustrates the construction procedure, which entails stacking the layers, adhering them, and adding steel and rubber reinforcing cords. In typical laminated elastomeric bearings, these cords are organized like steel plates to give vertical stiffness and prevent lateral bulging. The material and geometric characteristics of steel chords are listed in Table 1. The characteristics of the steel wires from the Bridgestone tires are listed in Table 1. A square-shaped STRP isolator with dimensions of 100 mm × 100 mm × 24 mm is used in this investigation. Table 2 shows that isolators having bonding percentages of 0%, 25%, 50%, 75%, and 100% with structural elements are referred to as STRP-0, STRP-25, STRP-50, STRP-75, and STRP-100, respectively. Table 2 contains detailed information on the specimens utilized in this investigation. Rubber modelling uses the Mooney-Rivlin model to characterize the nonlinear elastic behaviour of rubber precisely which shows in Table 3.

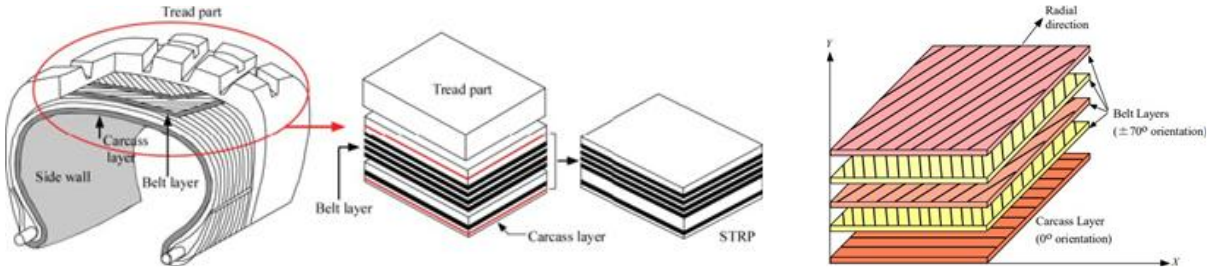

(a) (b)

Figure 1: STRP isolator: (a) Fabrication of STRP specimen; (b) Arrangement of steel reinforcing cords (Mishra, 2012)

Table 1: Properties of steel reinforcing cords (Zisan & Igarashi, 2021) (Hossain et al., 2024)

Layer	Poisson's ratio,υ	No. of filament	Filament dia (mm)	Steel cord area (mm^2)	Angle	Equivalent Thickness *tf* (mm)	Yield strength (GPa)	Modulus of elasticity *E*, (GPa)
Carcass	0.3	5	0.2	0.44	0°	0.40	2800	200
Belt	0.3	14	0.4	0.63	±70°	0.40	2800	200

Table 2: Geometric properties of STRP isolators

Model	Percentage (%) bond	Size (h×w×t) (mm)	Bonding area (mm)
STRP-0	0	100 × 100 × 24	0 × 0
STRP-25	25		50 × 50
STRP-50	50		71 × 71
STRP-75	75		87 × 87
STRP-100	100		100 × 100

Table 3: Mooney-Rivlin constants (Mishra, 2012)

C_{10}	C_{01}	C_{11}
0.40	1.22315	0.18759

3. FINITE ELEMENT (FE) MODELLING

The Marc Mentat program is used to model and analyse STRP isolators using finite elements (Marc, 2018) Because rubber can accurately model complex, nonlinear deformations under high-strain conditions, it is simulated as an isoperimetric element. The steel cord in the belt and the layers of the carcass are embedded in the rubber, which acts as the host material. Two separate pieces, as illustrated in Fig. 2(a)–2(c), are modelled to approximate partial bonding of the STRP with the isolator's top and bottom surfaces. STRP models with different bonding-area percentages are shown in this figure. The isolator's bottom surface, representing the building and foundation, is fixed in all dimensions, while the top surface is free to move in both vertical and horizontal directions. The finite element models of steel chords and STRP isolators with fine mesh are displayed in Figures 3(a) and 3(b), respectively. For every model, 5 MPa static axial stress is applied to the top surface. A complete finite element model with all boundary conditions is displayed in Figure 3(a). As seen in Fig. 3(d), the cyclic lateral displacement consists of six cycles corresponding to shear displacements of 25%, 50%, 100%, 150%, 200%, and 250%. This lateral displacement is applied in two orthogonal directions of the isolator, divided into six components according to the displacement's orientation. These components are oriented at 0° to 75° with 15° interval respect to the orthogonal direction. While the contact between

the unbonded portion of the isolator and building components is supposed to be a touched connection, the contact between rubber elements and bonded portions, as well as between building components and bonded parts, is assumed to be glued. For touch connections, a friction coefficient of 0.8 is used (Zisan & Igarashi, 2022). Finding the horizontal stiffness of these models are the main priority for this work.

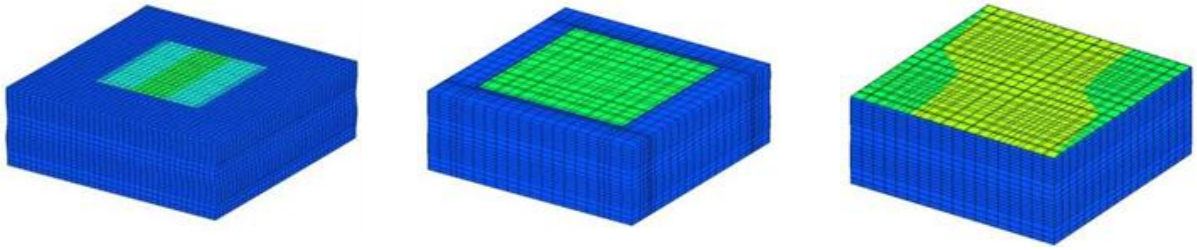

(a) 25% (b) 50% (c) 100%

Figure 2: Bonded portion of STRP: (a) STRP-0; (b) STRP-50; (c) STRP-100

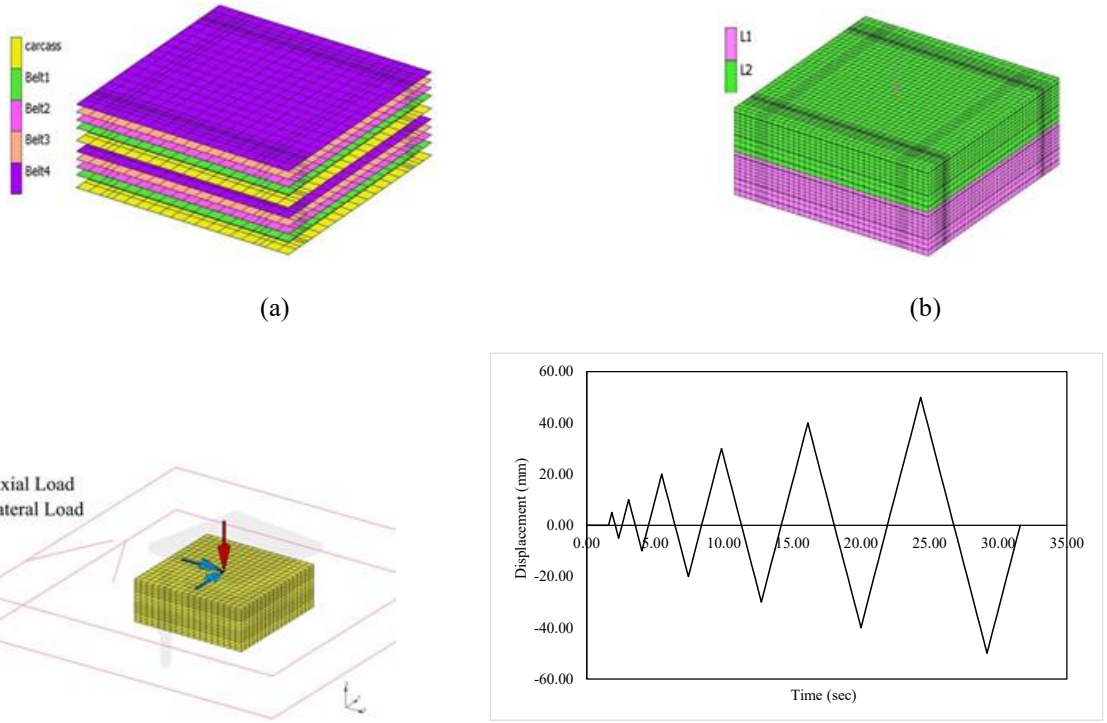

(a) (b)

(c) (d)

Figure 3: FE modelling of STRP : (a) Position of the embedded rebar components; (b) FE model mesh generation; (c) boundary conditions; (d) Lateral loading pattern

4. FINITE ELEMENT (FE) MODEL VERIFICATION

The FE model STRP-0 is confirmed through a comparison of the horizontal stiffness of the isolator, Ref. Model, as determined by Zisan and Igarashi (Zisan & Igarashi, 2022). Figure 4 illustrates that STRP-0 exhibits an average variance of 1.14% in horizontal stiffness in the Simultaneous action of applied displacement components in total, highest variation between performed model and reference model is 3.81% in total. Due to slight change of loading angle on a belt portion, 45° loading has shown some variation compared to reference model. The current study has employed an angle of ±70°, while the reference model used an angle of ±72°. The close correlation between Reference

model and Performed model indicates that the created finite element model is appropriate for subsequent parametric analysis.

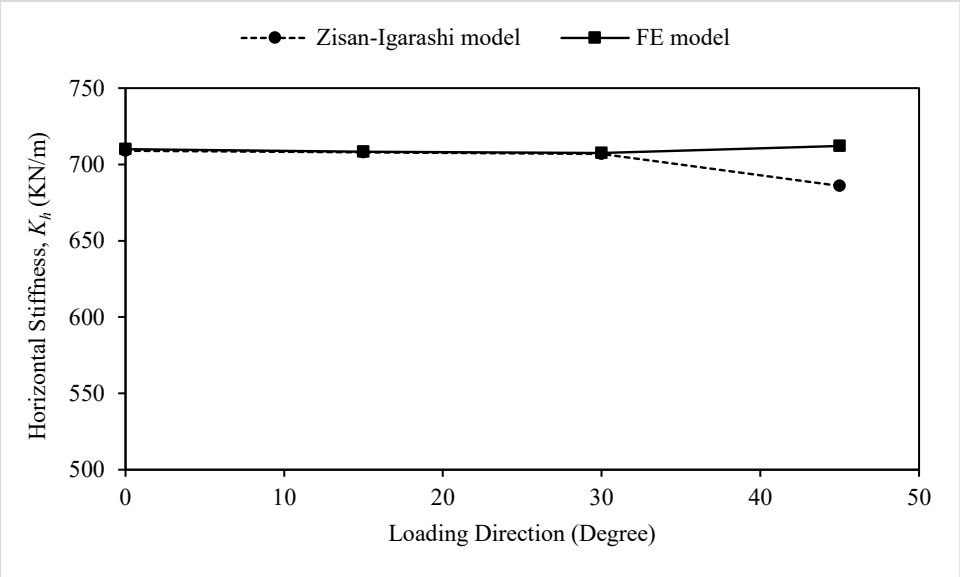

Figure 4: Validation of the FE model against the reference model

5. RESULTS AND DISCUSSIONS

5.1 Relationship between Force and Displacement

As individual loading direction has shown the same pattern for their individual bonded portion, that's why here only four curves are mentioned and also 25% bonded portion has shown almost same curve as 50% bonded portion for different loading direction. Figures 5 to 6 illustrate the cyclic lateral load response of STRP isolators with variable bond percentages subjected to shear displacements ranging from 25% to 250%, where loading angles of at loading angles of unbonded at 15° for Y direction, 50% bonded at 30° loading for X direction, 75% bonded at Y Axis and 100% bonded at X Axis direction for 45º Loading has been shown. And The data indicates that under static stress circumstances, all isolators exhibit stability, with no slippage observed in the completely unbonded STRP isolator as all curve complete their full cycle. The horizontal stiffness derived from these hysteresis curves are detailed in the subsequent section.

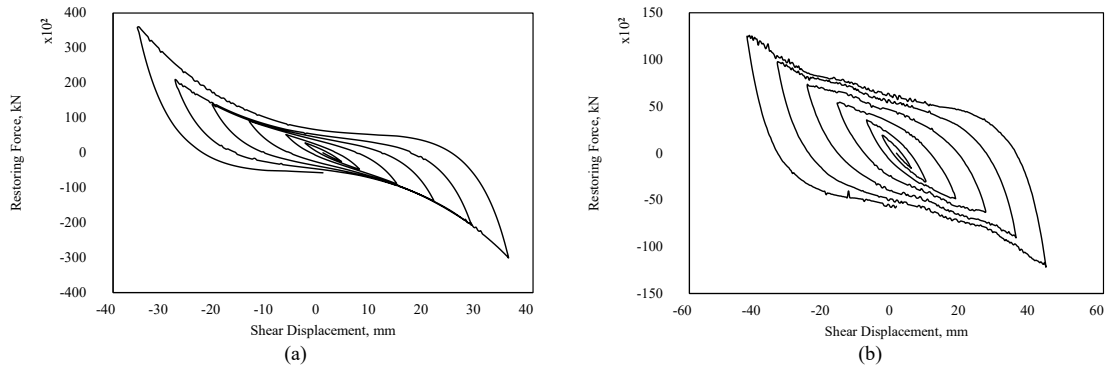

Figure 5: (a) Un-Bonded Y Axis hysteresis curve at 15º Loading; (b) 50% Bonded X Axis hysteresis curve at 30º Loading

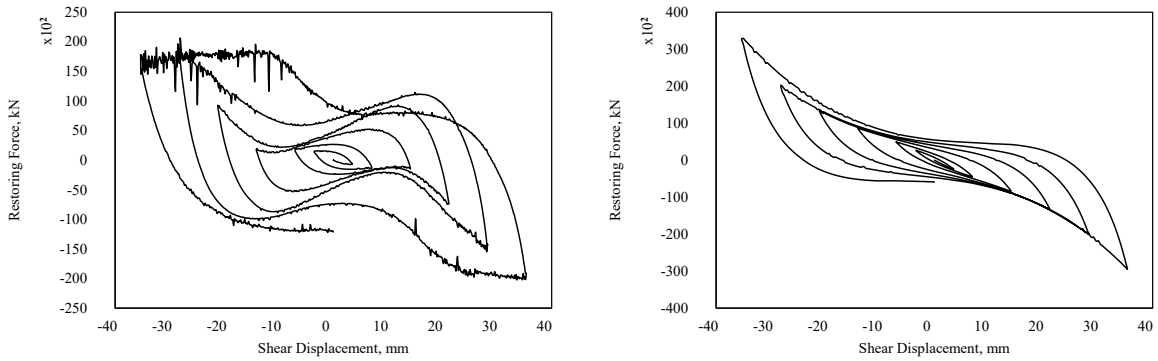

Figure 6: (a) 75% Bonded Y Axis hysteresis curve; (b) 100% Bonded X Axis hysteresis curve at 45º Loading

5.2 Horizontal Stiffness

The horizontal stiffness (K_h) of the STRP isolator is determined using the subsequent formula (ASCE/SEI 7-10, 2010):

$$K_h = \frac{F^+ - F^-}{u^+ - u^-} \tag{1}$$

Figures 5 and 6 illustrate the shear displacement (mm) at which the STRP isolators can experience strains of up to 250% and has shown in tables 4 to 9. In this context, F^+ and F^- represent the highest positive and negative forces on the hysteresis curve, corresponding to the maximum positive displacement, u^+, and the maximum negative displacement, u^-, respectively. The horizontal stiffness values of STRP isolators are presented in Tables 4 to 9. Figure 7 and 8 illustrates the relationship between highest and lowest stiffness and with loading direction. The rigidity diminishes as the bonded area between the isolator and structural components expands. At a 45° orientation, STRP-50 exhibits the lowest stiffness which is 385.32 KN/m, signifying enhanced flexibility and optimal isolation efficacy. However, as the bonding area expands, the stiffness value diminishes progressively; this trend alters around 75% bonding, where it begins to grow. Additionally, lateral stiffness declines with an initial rise in lateral displacement, but approximately at 150% shear displacement, it starts to increase. The STRP-100 demonstrates superior horizontal rigidity and maximum has seen for 60° loading direction which is 1306.82 KN/m.

Table 4: Horizontal Stiffness for STRP models at 0 degree

Shear Displacement (%)	STRP-0 K_h (KN/m)	STRP-25 K_h (KN/m)	STRP-50 K_h (KN/m)	STRP-75 K_h (KN/m)	STRP-100 K_h (KN/m)
25	1053.39	883.45	622.14	660.81	1070.92
50	932.13	791.16	588.47	612.66	984.15
100	710.13	702.14	467.14	550.37	886.77
150	864.55	705.45	442.34	622.45	914.21
200	927.76	695.74	457.77	832.88	1028.02
250	1072.81	754.11	443.12	894.75	1285.42

Table 5: Horizontal Stiffness for STRP models at 15 degree

Shear Displacement (%)	STRP-0 K_h (KN/m)	STRP-25 K_h (KN/m)	STRP-50 K_h (KN/m)	STRP-75 K_h (KN/m)	STRP-100 K_h (KN/m)
25	1032.93	875.42	598.31	637.42	1060.81
50	907.58	772.41	560.32	590.37	975.19
100	708.35	691.17	440.48	524.55	861.32
150	774	694.44	408.78	601.74	869.73
200	852.2	683.52	432.64	817.64	953.41
250	879.49	743.67	427.87	870.33	1028.32

Table 6: Horizontal Stiffness for STRP models at 30 degree

Shear Displacement (%)	STRP-0 K_h (KN/m)	STRP-25 K_h (KN/m)	STRP-50 K_h (KN/m)	STRP-75 K_h (KN/m)	STRP-100 K_h (KN/m)
25	1020.64	862.13	578.22	623.51	1070.98
50	927.48	752.83	532.13	572.36	983.95
100	707.64	677.52	422.19	512.14	885.11
150	768.51	674.72	395.36	591.44	912.014
200	797.72	663.41	416.11	801.44	1006
250	828.13	731.67	409.77	858.45	1099.45

Table 7: Horizontal Stiffness for STRP models at 45 degree

Shear Displacement (%)	STRP-0 K_h (KN/m)	STRP-25 K_h (KN/m)	STRP-50 K_h (KN/m)	STRP-75 K_h (KN/m)	STRP-100 K_h (KN/m)
25	1012.74	841.36	600.16	610.78	1068.77
50	915.42	741.83	544.8	551.43	981.17
100	712.13	657.15	438.86	492.02	882.75
150	746.34	644.72	413.36	575.16	912.21
200	787.14	647.54	389.66	791.39	1026.02
250	819.67	712.25	385.32	846.23	1284.34

Table 8: Horizontal Stiffness for STRP models at 60 degree

Shear Displacement (%)	STRP-0 K_h (KN/m)	STRP-25 K_h (KN/m)	STRP-50 K_h (KN/m)	STRP-75 K_h (KN/m)	STRP-100 K_h (KN/m)
25	1012.34	864.11	584.59	622.55	1061.39
50	924.74	744.55	546.02	542.65	979.89
100	700.16	672.15	425.11	511.31	879.26
150	759.65	680.11	395.11	614.44	903.85
200	790.14	657.11	419.29	807.44	1016.45
250	832.14	737.12	413.61	879.45	1306.82

Table 9: Horizontal Stiffness for STRP models at 75 degree

Shear Displacement (%)	STRP-0 K_h (KN/m)	STRP-25 K_h (KN/m)	STRP-50 K_h (KN/m)	STRP-75 K_h (KN/m)	STRP-100 K_h (KN/m)
25	1022.22	862.34	581.73	619.89	1053.34
50	900.45	743.7	540.44	540.97	966.75
100	700.12	668.74	425.34	529.46	861.47
150	762.14	682.31	396	601.47	869.57
200	831.74	662.54	417.77	805.22	915.67
250	881.44	735.45	411.74	872.11	1226.13

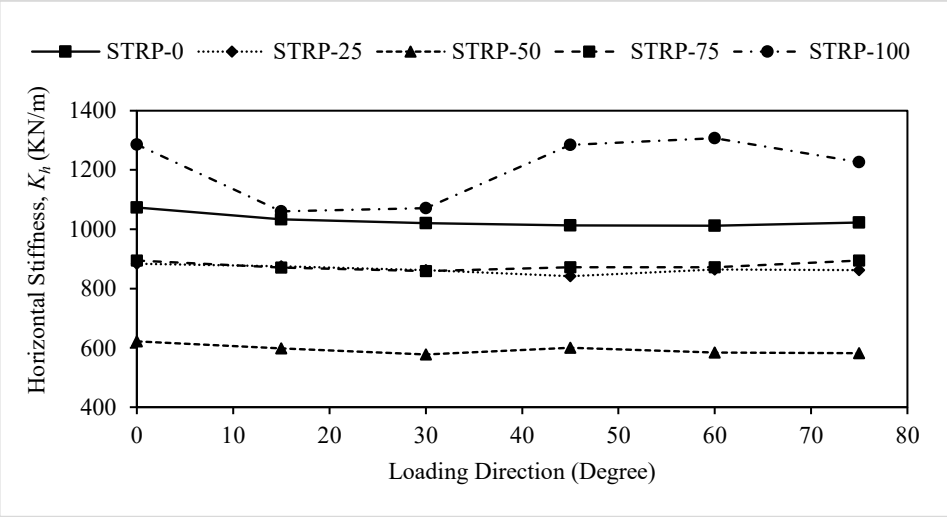

Figure 7: Highest Horizontal Stiffness for STRP

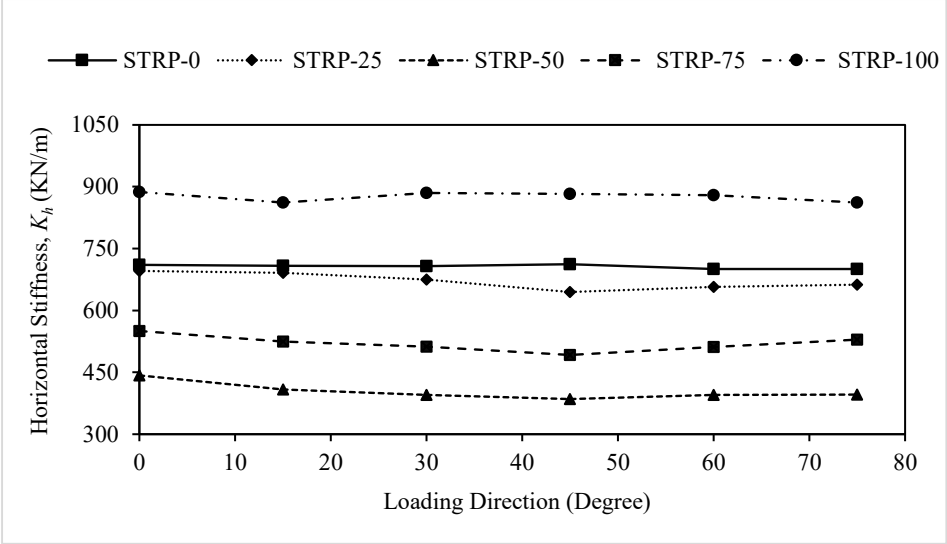

Figure 8: Lowest Horizontal Stiffness for STRP

6. CONCLUSIONS

This study examines the lateral load performance of STRP isolators with differing bonding areas between the isolator and structural levels under cyclic bi-directional lateral stress. Only square-shaped isolators exposed to cyclic loads at orientations ranging from 0° to 75° in 15° increments are evaluated. The principal conclusions are as follows:

- STRP-50 (partially bonded) demonstrates superior efficacy in seismic isolation for this criterion; however, its efficiency diminishes when the number of bonded connections between the isolator and structural components increases.
- Additionally, STRP-0 and STRP-25 exhibit greater rigidity than STRP-50. Initially, from STRP-0 to STRP-50, stiffness diminishes with the addition of the bonded portion; but, from STRP-75 to STRP-100, it increases with the bonded portion. The STRP-100 (totally bonded) isolator exhibits the lowest seismic isolation efficacy due to its highest lateral stiffness.
- Unbonded STRPs maximum lateral stiffness has been found for 0° loading direction which is 1072.81 KN/m and minimum is 700.12 KN/m at 75° loading.
- The minimum lateral stiffness for STRP-25 is 644.72 KN/m at a 45° loading direction, while the maximum lateral stiffness is 883.45 KN/m at a 0° loading direction.

- STRP-50 has a maximum lateral stiffness of 622.14 KN/m at a 0° loading direction and a minimum lateral stiffness of 385.32 KN/m at a 45° loading direction.
- STRP-75 has a minimum lateral stiffness of 492.02 KN/m at a 45° loading direction and a maximum lateral stiffness of 894.75 KN/m at a 0° loading direction.
- STRP-100 has a maximum lateral stiffness of 1306.82 KN/m at a loading direction of 60° and a minimum lateral stiffness of 861.32 KN/m at a loading direction of 15°.
- The maximum lateral stiffness has seen in the fully bonded section under 60° loading at 250% shear displacement which is 1306.82 KN/m, on the other hand, the minimum has been recorded at 45° loading at the same shear displacement at STRP-50 which is 385.32 KN/m.

DECLARATION OF USE OF AI

The authors state that only language editing and paraphrasing to enhance readability and clarity were done using AI-based techniques (QuillBot). The research approach, data collecting, analysis, and interpretation did not make use of any AI techniques.

REFERENCES

Marc-Mentat, MSC. (2018). Theory and user information, Vol. A, Santa Ana, CA: MSC Software Corporation.

Hossain, M.M., Zisan, M.B., Maher, S.K., & Abdullah, N. (2024). "Effect of Loading Directionality on Seismic Behavior of Partially Bonded Square-Shaped Scrap Tire Rubber Pad Isolator,". *Proceedings of the 7th International Conference on Advances in Civil Engineering (ICACE2024)* (pp. 2471–2478). Chattogram: 7th International Conference on Advances in Civil Engineering (ICACE2024).

Mishra, H.K. (2012). *"Experimental and Analytical Studies on Scrap Tire Rubber Pads for Application to Seismic Isolation of Structures".* Kyoto: Kyoto University, Japan.

Kalfas, K.N., Mitoulis, S.A., & Konstantinidis, D. (2020). "Influence of Steel Reinforcement on the Performance of Elastomeric Bearings,. *Journal of Structural Engineering*, Volume 146, Issue 10.

Turer, A., & Özden, B. (2007). "Seismic Base Isolation Using Low-Cost Scrap Tire Pads (STP)," . *Materials and Structures*, 891–908.

Zisan, M.B., & Igarashi, A. (2022). A hysteresis force model for unbonded scrap tire rubber pad isolators,. *3rd International Conference on Natural Hazards & Infrastructure.* Greece, Athens: 3rd International Conference on Natural Hazards & Infrastructure.

Zisan, M.B., Haque, M.N. & Hasan, M.A. (2022). Seismic vulnerability assessment of masonry building supported by STRP isolators. *Asian Journal of Civil Engineering*, 1-16.

Zisan, M.B., & Igarashi, A. (2021). "Evaluation of unbonded Strip-STRP bearing based on current design guidelines,". *IABSE Congress – Resilient technologies for sustainable infrastructure*, 1247-1256.

Zisan, M.B., & Igarashi, A. (2022). "Effect of Loading Directionality on the Horizontal Stiffness of Unbonded Scrap Tire Rubber Pad Isolator.". *6th International Conference on Advances in Civil Engineering. ICACE 2022.* Chattogram: ICACE 2022.